Electronic Supplementary Material (ESM) for:

Come on baby, let's do the twist: the kinematics of killing in loggerhead shrikes

Diego Sustaita, Margaret A. Rubega, and Susan M. Farabaugh

Text S1. Details of kinematic analysis of electronic supplementary materials video S1, as presented in figure 1 of main text.

We could not affix external markers to shrikes, and therefore we tracked the few features we could reliably and consistently identify on the shrike's head (the dorsocranial base of the beak and upper and caudal-most points of the facemask on either side of the head), mouse's head (tip of the rostrum), and mouse's body (at the intersection of the tail and rump) (figure S1 (a, b)) using imageJ [1]. The pivot-point for the angular measurements at the dorsocranial base of the shrike's beak was often approximated by the vertex formed by the anterior convergence of the left and right sides of the black facemask. The shrike's head angle was determined by the movement of the right side of the facemask. When the right side was occluded (or the edge of the mask was indecipherable), we reflected the angle of the left side based on our average measurement of 93.5° for the angular deviation between the left and right margins of the facemask (from the base of the beak) when viewed head-on.

We estimated our tracking precision by calculating the standard deviations of the marker-marker distances across frames [2] for the shrike's and mouse's heads, assuming that these segment lengths should remain relatively unchanged, save for tracking error and/or deviations from A 2D-planar view. For example, the standard deviation of marker-marker distances for a static line drawn along the baseboard of the feeding corral near the shrike was 0.04 cm, amounting to 0.12% of its mean length across frames. The values for the shrike's and mouse's heads were 0.34 cm and 0.25 cm (averaged over 5 repeated measures), respectively, amounting to ~8-12% of their mean lengths, reflecting considerable tracking error and/or deviations from planarity. Although these values are not ideal, the observed deviations should not substantially affect the resultant segment angles (below).

We obtained the angles of the lines between the dorsocranial base of the beak and the shrike's head, mouse's rostrum, and mouse's rump, relative to the frame horizon using the "ATAN" function in Microsoft Excel (2010) (figure S1 (c)). One of us (DS) digitized the 64-frame sequence five separate times (each time with frames in random order), calculated angular velocities and accelerations, and estimated g-forces and torques for each repetition (data S2) to obtain error variances that incorporates both landmark positional errors and digitization noise. In the main text we report the mean ± s.d. of the peak absolute values of ω, α, τ, and g-forces calculated from each repetition. From the standard deviation of the angles of the endpoints of a line marked on the floor of the feeding corral (described above), we estimate that digitization noise (but not necessarily landmark positional error) falls within the range ±0.064°.

We smoothed the data using a 4th-order zero phase shift low-pass Butterworth filter with a cut-off frequency of 30 Hz [3], using [4], then mean-centered the final values depicted in figure 1 of the main text.

Four additional attack sequences (one by the shrike measured above, plus three other individuals) afforded the opportunity to estimate average angular velocities (ω_{avg}) from the time required to complete an ~90° turn of the head (i.e., 1.57 rad/time [s] based on number of frames), since we could assess this from non-planar camera angles. The head oscillation frequencies from these same attack sequences averaged (± s.d.) 10.3±2.5 Hz. We also measured the attack from the more detailed analysis (above) in this manner, producing a data set of n = 5 to test the correlation between head oscillation frequency and ω_{avg}. We found a significant correlation (r = 0.90, P = 0.036) between the two, suggesting broader generality to the larger sample of shrikes for which we measured head oscillation frequencies, beyond the four individuals for which we obtained direct measurements of ω *and* ω_{avg}.

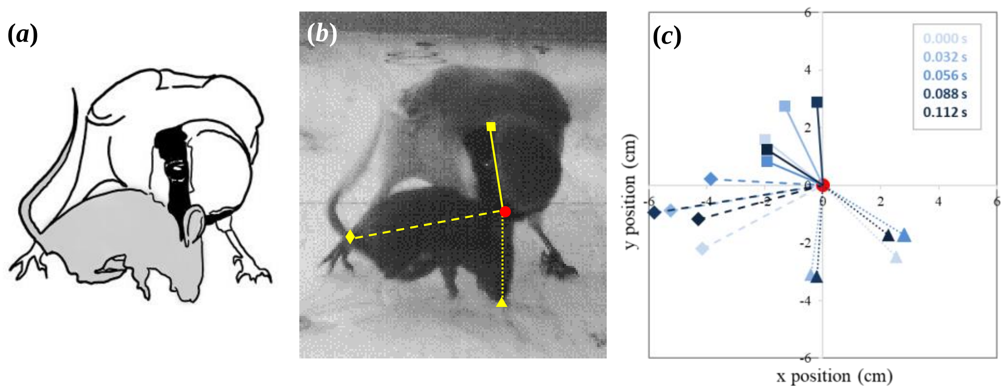

Figure S1. (*a*) Schematic illustrating bite point on neck of mouse (behind ear) for clarity. (*b*) Landmarks used to track angular changes over time in the shrike's head (squares and solid lines), the mouse's head (triangles and dotted lines), and the mouse's body (diamonds and dashed lines) about the dorsocranial base of the beak (red dot) for a selected frame (at 0.088 s). (*c*) 2D coordinates of landmarks and angular changes of one full head-rolling cycle (symbols and lines darken over time). Note that the line segments here are anchored to a fixed central point (0,0) for clarity; in actuality, angles of unanchored lines were measured such that both endpoints were free to vary.

Text S2. Additional details of torque and g-force estimates.

Torque and moment arm:

We estimated rotational torque (τ) from the product of the peak angular acceleration we observed (α) and the moment of inertia (I) of a mouse the size of the one in the video, which in turn was extrapolated from published values of the moment of inertia of the center of mass (I_{CM}) for mice across a range of body sizes, determined empirically by swinging them from a pendulum [5]. Because *I* is sensitive to object shapes and center of mass [6], we felt this approach would provide a more accurate estimate since it did not require us to assume any particular shape (or center of mass) for the mouse in the video. We can obtain an estimate of the moment arm (r) implicit to this calculation, from:

$$\tau = F_t \times r = m \times r^2 \times \alpha \text{ [2]},$$

Based on our estimated peak instantaneous rotational torque (τ) of 0.022 N·m, an m (mouse's mass) of 0.0173 kg, an α (observed peak instantaneous angular acceleration) of 2696.1 rad·s^{-2}, r = 0.0217 m.

To then relate our observed peak instantaneous torque estimate of 0.022 N·m to the mean tensile failure force of 2.45 N for cervical facet capsular ligaments of rats reported by [7], we performed the following calculation:

We do not know the exact bending moment for the cervical spine of a mouse whilst being shaken by a shrike. Therefore, to turn this value into a torque, we estimated a moment arm (d) of a length approximately equal to the dorsoventral depth of the vertebral centrum (based in part on [8]) of 2.1 mm (0.0021 m) from Fig. 1B of [7] using imageJ [1].

We then made the simplifying assumption that during prey-shaking motion, the ~2.45 N of tensile force (F_t) required for the ligament to rupture would be generated by the angular acceleration of one vertebra rotating away from another, about a pivot at one end of the junction of two adjacent vertebral centra (as though the vertebral column was snapped apart between two vertebrae like a twig; figure S2). In this scenario, the *minimum* torque required to generate the requisite tensile force would be 2.45 N × 0.0021 m = 0.0051 Nm, which is 4.3 times less than the torque we estimated from prey-shaking, above. Below we diagram (not to scale) the abovementioned torques, as we perceive to have estimated them (figure S2).

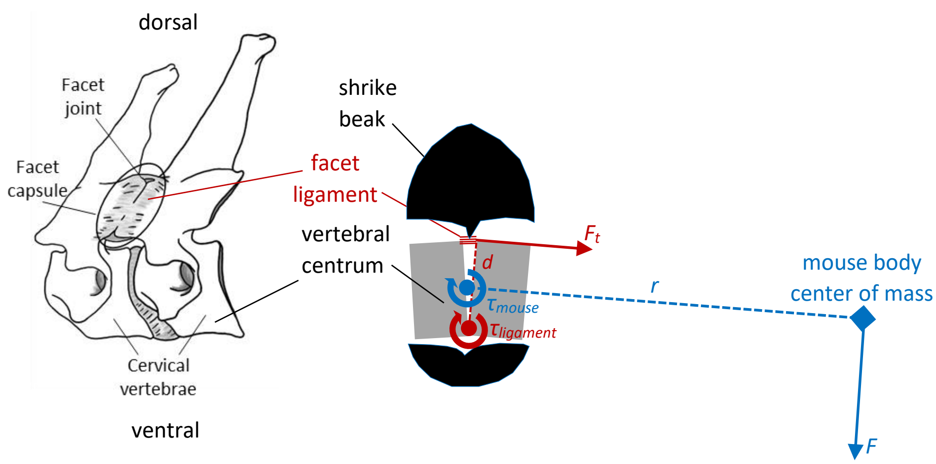

Figure S2. Image of a human cervical vertebra (redrawn from [9]) showing the cervical facet capsular ligaments in the context of the forces to which those of mice might be exposed during prey-shaking by shrikes (not diagramed to scale). The symbols in blue depict the torque (τ_{mouse}), moment arm (r), and tangential force (F) measured for the mouse's body from video S1. The symbols in red depict the torque ($\tau_{ligament}$) we estimated from the tangential force (F_t) given by [7], and our estimate of the moment arm (d) from Figure 1B of [7]. Naturally, this calculation assumes that the point of bending occurs between two successive vertebrae and the rest of the spine and body remain rigid; in reality, however, the bending moments of the cervical spine under these conditions are far more complex.

G-force:

(1) We computed angular accelerations (α) from the second derivative of shrike head, mouse head, and mouse body angles over time. (2) We then calculated total instantaneous (linear) acceleration for non-uniform circular motion (a) as the vector sum of a_t (tangential) + a_c (centripetal), where $a_t = r \times \alpha$, $a_c = r \times \omega^2$ [6], and $r = 0.0217$ m (from above). Finally, we derived g-forces by dividing a by the gravitational acceleration constant 9.80655 $\mathrm{m \cdot s^{-2}}$.

To corroborate this estimate, we also performed a different calculation used for determining g-forces of centrifuges: $g = 1.118 \times 10^{-5} \times \mathrm{R} \times \mathrm{S}^2$, where R = radius of rotor in cm and S = speed in rotations per minute (http://tools.thermofisher.com/content/sfs/brochures/TR0040-Centrifuge-speed.pdf). Using the observed cycle frequency of the mouse's body of ~4 cycles/0.5 s = 8 Hz = 480 rpm, and the 2.146 cm radius from above, yields:

$$g = 1.118 \times 10^{-5} \times 2.17 \text{ cm} \times (480 \text{ rpm})^2 = 5.6\, g.$$

References

1 Rasband WS. 1997-2011 *ImageJ*. Version 1.44p. Bethesda: U. S. National Institutes of Health.

2 Brainerd EL, Baier DB, Gatesy SM, Hedrick TL, Metzger KA, Gilbert SL, Crisco JJ. 2010 X-ray reconstruction of moving morphology (XROMM): precision, accuracy and applications in comparative biomechanics research. *J Exp Zool A Ecol Genet Physiol* **313**, 262-279.

3 Winter DA. 2009 *Biomechanics and Motor Control of Human Movement*. New Jersey: John Wiley & Sons, Inc.

4 Van Wassenbergh S. 2007 Fourth-order, zero phase-shift Butterworth low-pass filter & adaptive butterworth filter. Version 2: https://www.uantwerpen.be/en/staff/sam-vanwassenbergh/my-website/excel-vba-tools/).

5 Walter RM, Carrier DR. 2002 Scaling of rotational inertia in murine rodents and two species of lizard. *J. Exp. Biol*. **205**, 2135-2141.

6 Wilson JD, Buffa AJ. 1997 *College physics, 3rd ed*. Prentice Hall, Upper Saddle River, NJ.

7 Quinn KP, Winkelstein BA. 2007 Cervical facet capsular ligament yield defines the threshold for injury and persistent joint-mediated neck pain. *J. Biomech*. **40**, 2299-2306.

8 Le Huec J-C, Richards J, Tsoupras A, Price R, Léglise A, Faundez AA. 2018 The mechanism in junctional failure of thoraco-lumbar fusions. Part I: Biomechanical analysis of mechanisms responsible of vertebral overstress and description of the cervical inclination angle (CIA). *Eur Spine J* **27** (Suppl 1), S129–S138.

9 Brownstein SP, Puglisi BF. 2016 Evaluation of cervical capsular ligament injuries following whiplash injury. *Ortho & Rheum Open Access J*. **2**: 555599. DOI: 10.19080/OROAJ.2016.02.555599.